Dynamics of triple lines at soft interfaces

H. Gérardin, E. Verneuil, A. Constant, S. Dubois, J. Clain, X. Noblin,
A. Buguin and F. Brochard-Wyart

Laboratoire de Physico-Chimie Curie, Institut Curie, CNRS UMR 168
11 rue Pierre et Marie Curie, 75248 Paris Cedex 05, France

Abstract. – A rubber cylinder (R) is pressed against a glass plate (S) through a liquid drop (L). The liquid film, entrapped between R and S, dewets and a R/S dry contact, consisting in a band bordered by two straight contact lines, is formed. A row of equally spaced defects, graved on the glass plate, is used to pin and to deform periodically the R/L/S triple line. We observe the relaxation of this line by interference microscopy and we study the relaxation time *vs.* the period of the defects, the viscosity of the liquid, for hard and soft rubbers. A naive model, based on the balance between elastic and viscous forces, gives a plausible picture for these observations.

Introduction. – Static and dynamics of solid/liquid/air S/L/A contact lines have been widely studied both theoretically [1–4] and experimentally [5–13]. Joanny and de Gennes [1] showed the unusual structure of the line elasticity: if the line undulates in space with a wave vector q and an amplitude u_q, the elastic energy F_{el} is proportional to $|q|$ rather than the classical quadratic expression. In fact, L/A interface distortions give an energy proportional to q^2 but integrated over the penetration length of the deformation ($\sim q^{-1}$), this leads to an energy F_{el} linear in q. This unusual elasticity has been named "fringe elasticity" [3] and exhibits unusual properties. In particular, the profile of the line deformed by a localized force is logarithmic (and not made of two straight lines as in the case of an elastic string). For these S/L/A systems, the dynamics of line fluctuations has been studied in both viscous [4–6] and inertial regimes [12, 13].

In the present paper we focus on the case of solid/liquid/rubber (S/L/R) triple lines. Here the deformation energy is a combination of capillary energies and elastic energies inside the rubber (of Young modulus E). Thus the wetting features of a liquid, intercalated between a rubber and a passive solid are controled by two major parameters:

i) The spreading parameter $S = \gamma_{SR} - (\gamma_{SL} + \gamma_{LR})$ (where γ_{ij} are, respectively, the interfacial energies between S/R, S/L and L/R). We focus our attention on situations of *negative S*, where a liquid drop does not spontaneously wet the contact.

ii) The "elastic length" $h_0 = |S|/E$. At spatial scales larger than h_0, elastic energies are dominant in the rubber. For instance a drop, of size $\gg h_0$, at the solid/rubber interface, is
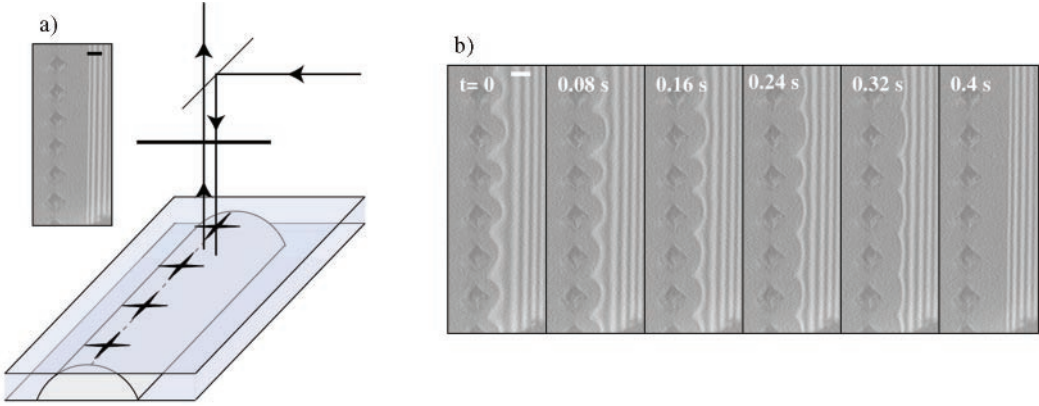
Fig. 1 – (a) Schematic representation of the experimental set-up. Inset: RICM image of the rectangular S/R contact bordered by a S/L/R triple line. The black bar represents $10\,\mu$m; (b) Pictures of a S/L/R triple line at different times during the relaxation: thanks to a quick motion, the indents row (period is $20\,\mu$m) generates triple-line sinusoidal undulations at the cylinder edge. The viscosity of the liquid is $\eta = 0.471\,$Pa s and the Young modulus of the elastomer is $E = 0.8\,$MPa. The white bar represents $10\,\mu$m.

not spherical, but has the shape of a flat penny, with a thickness H and a radius R. The scaling law relating H and R is $R \sim H^2/h_0$ [14,15]. Near the triple line (a circle of radius R) the static profile $z_0(x)$ is of the form

$$z_0(x) \cong (h_0 x)^{1/2} \tag{1}$$

this is very different from the standard capillary behavior, where we would have $z \approx x$. For our system h_0 is small but sizeable ($h_0 \approx 10\,$nm).

To study R/S/L triple lines, we form an adhesive band by pressing a rubber cylinder against a glass plate through a non-wetting liquid (fig. 1). A film is squeezed at the R/S interface. It thins by drainage and suddenly dewets. The dynamics of dewetting at soft interfaces has been intensively studied since the pioneer works of Roberts [16] with both viscous liquids [14,15,17] and water [18], and interpreted in ref. [19] by a transfer of surface energy into viscous dissipation in the liquid. After dewetting, the dry contact consists in a band limited by two triple lines. We deform the triple line (y-axis in fig. 1a) by using a row of defects, graved periodically on the glass substrate and we observe the dynamics of relaxation.

Materials. – The *rubber* is a commercial elastomer prepared by cross-linking an end-functionalized poly-dimethylsiloxane (PDMS) supplied in two liquid parts (Sylgard 170 A&B, Dow Corning). The Young modulus of this elastomer can be adjusted by varying the weight proportions of the A : B compounds before reticulation. After curing, we get rubbers whose elastic modulus (measured by classical JKR tests) fall in two groups: "hard" rubber ($E \simeq 0.8\,$MPa) for A : B ranging from 70 : 30 to 50 : 50, and "soft" rubber ($E \simeq 0.2\,$MPa) for 75 : 25 or 80 : 20. To make cylindrical elastomers, we first grave (with a glass knife) two parallel grooves on a non-wettable surface (a fluorinated glass slide). The liquid PDMS is then poured between the grooves (that give to the liquid a cylindrical shape by trapping the triple line) and reticulation is obtained after curing (65 °C for two days). We get half-cylinders (radius $\approx 1\,$mm, length $\approx 1\,$cm). As *solid substrates*, we use glass slides chemically modified to obtain low surface energies. Slides are silanated with octadecyltrichlorosilane following

classical methods [20, 21]. Before the silanisation, we print in the glass periodically spaced diamond indents as performed by Martin [17]. The typical size of these indents is $10 \, \mu m$ and we vary the period from 20 to $60 \, \mu m$. For the *liquids*, we use fluorinated silicone oils (PFAS) with dynamic viscosities η ranging between $0.47 \, Pa \, s$ and $3.02 \, Pa \, s$ at $20 \, °C$. These liquids are purchased from Roth-Sochiel in three different viscosities and we mix them to get intermediate viscosities without significative change of the spreading parameter S.

Triple-line modulation and observation. – The rubber cylinder is deposited on a dark substrate (to avoid extra reflections) which is set on the mobile stage of an upright microscope (fig. 1a). The silanated glass slide is set to a three-axis micromanipulator. We approach the slide normally to the rubber cylinder through a PFAS drop. The R/L interface is observed by interferencial microscopy. The monochromatic illumination is provided by a halogen lamp and an interference filter ($\lambda = 546 \, nm$) through a 40x objective. Interfaces are monitored with a standard video camera (fig. 1b). We first squeeze the rubber cylinder on the glass slide: as shown in fig. 1a, a rectangular contact is established after dewetting. We slowly translate the cylinder to superimpose the triple line and the row of defects. At time $t = 0$, we suddenly move the row of defects under the elastomer: the triple line is pinned and undulates. Then we measure the profile of the triple line during relaxation. Figure 1b shows a typical sequence of images taken during this relaxation. We observe a dominant wavelength imposed by the indents periodicity.

Measurement of the relaxation time τ_q. – The shape of the triple line is not purely sinusoidal: it is composed of various sinusoidal harmonics which relax at different velocities. To extract the first harmonic (imposed by the periodicity of the defects), we binarise the pictures and we perform the Fourier transform of the triple-line contour. We denote u_q the Fourier transform amplitude associated to the wave vector q. For each spectrum, we collect the amplitude u_q for the first harmonic (fig. 2a) (for higher harmonics the amplitude is usually too small). The amplitude of a given q-peak follows an exponential decay *vs.* time (fig. 2b): $u_q = u_{q_0} \exp[-(t - t_0)/\tau_q]$, which gives the relaxation time τ_q.

We have explored *wave vectors* ranging from 0.017 to $0.1 \, \mu m^{-1}$ for fixed values of the liquid viscosity ($\eta = 0.47 \, Pa \, s$) and of elastomer elastic modulus ($E = 0.8 \, MPa$). This range is very limited for two reasons: on the one hand, for small wavelengths the amplitude of the triple-line deformation becomes too small to be measured with accuracy using an optical microscope. On the other hand, for large wavelengths, there are no more interactions between neighboring defects, and each of them can be seen as an isolated perturbation. Nevertheless, a log-log plot (fig. 2c) of the characteristic relaxation time for the main harmonic *vs.* q permits to predict a trend concerning its influence. We obtain $\tau_q \approx q^{-1.2 \pm 0.3}$.

We have used the same strategy to follow the dynamics of relaxation *vs.* the liquid viscosity η and the elastic modulus E. We have varied the liquid viscosity from $\eta = 0.47 \, Pa \, s$ to $\eta = 3.07 \, Pa \, s$ (with $E = 0.8 \, MPa$ and $q = 0.05 \, \mu m^{-1}$). For the main harmonic, the relaxation time τ_q as a function of liquid viscosity η is reported in the log-log plot in fig. 2d. It gives $\tau_q \approx \eta^{1.1 \pm 0.3}$ showing that τ_q is roughly proportional to the liquid viscosity η. We have repeated the experiment with "hard" and "soft" rubbers by keeping constant the liquid viscosity ($\eta = 0.47 \, Pa \, s$) and the indents wave vector ($0.05 \, \mu m^{-1}$). We find a relaxation time $\tau = 110 \, ms$ for the hard rubber ($E = 0.8 \, MPa$) and $\tau = 70 \, ms$ for the soft one ($E = 0.2 \, MPa$). Note this surprising feature that the "softest" elastomers relax more quickly. Unfortunately, the elastic modulus does not vary continuously with composition and we have only two values for E.

To summarize, these observations show that the characteristic relaxation time of the S/L/R triple line is an increasing function of the liquid viscosity and of the wavelength of the applied deformation, and decreases as the Young modulus increases.
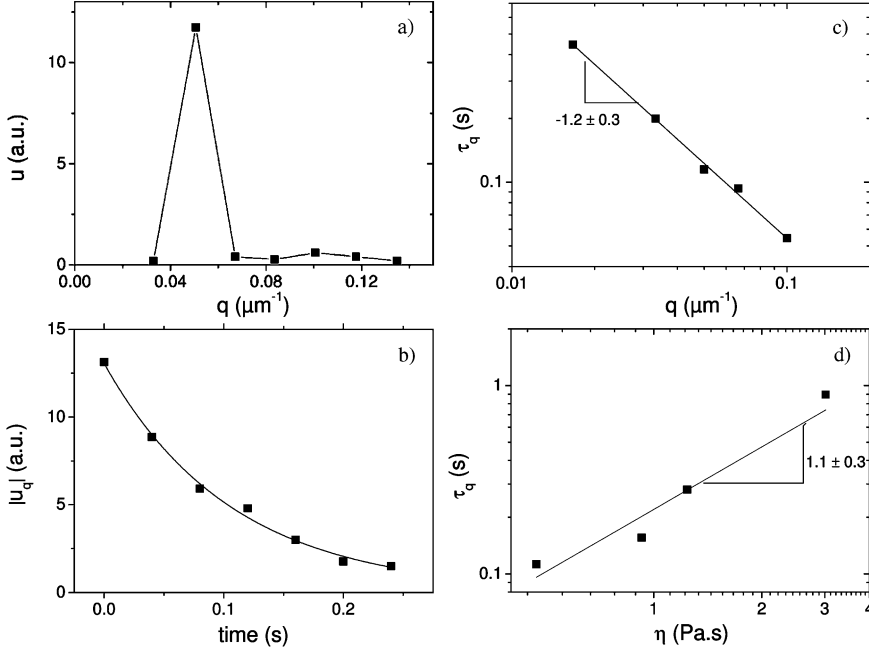
Fig. 2 – Dynamics of relaxation: (a) u_q spectrum; (b) $u_q(t)$ relaxation: an exponential fit gives the relaxation time τ_q; (c) triple-line relaxation time τ_q *vs.* wave vector q (log-log plot) for $\eta = 0.47\,\mathrm{Pa\,s}$ and $E = 0.8\,\mathrm{MPa}$; (d) τ_q *vs.* η (log-log plot) for $q = 0.05\,\mu\mathrm{m}^{-1}$ and $E = 0.8\,\mathrm{MPa}$.

Interpretation. – We propose here a scaling estimate of the relaxation time τ_q incorporating elastic effects in the rubber and viscous friction in the fluid slab (of thickness $z(x)$). The critical assumption is that the perturbation extends over a width $\Delta x \approx q^{-1}$ (comparable to the wavelength of the modes along y). This is a natural assumption since both the elastic and the viscous fields are controlled by Laplacian equations.

a) Elasticity. A first approximation to the slit profile $z(x)$ is a simple displacement from the unperturbed, static form $z_0(x) \cong (h_0 x)^{1/2}$. If we call u the amplitude of the line deformation $u(y) = u_q \cos 2\pi(qy)$ (fig. 3), it gives

$$z(x,y) \cong z_0(x + u(y)) \cong z_0(x) + u\frac{\partial z_0}{\partial x}\,. \tag{2}$$

The resulting deformations are of order

$$\varepsilon = \left|\frac{\partial z}{\partial y}\right| = qu_q\frac{\partial z_0}{\partial x} \tag{3}$$

and the over all elastic energy (integrated over x and z, $\Delta x \approx \Delta y \approx q^{-1}$, in the rubber) per unit length in the y-direction is

$$F_{el} = \int \frac{1}{2}E\varepsilon^2 \,\mathrm{d}x\,\mathrm{d}z \cong Eh_0 u_q^2 q. \tag{4}$$

Thus F_{el} is comparable to the capillary energy $\frac{1}{2}\gamma q u_q^2$ (as would be expected, since the profile minimizes the sum of both).
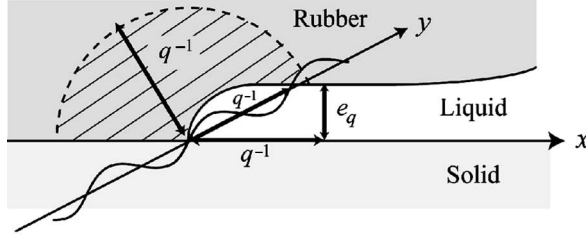
Fig. 3 – A modulation of the line induces a deformation of the rubber and of the R/L interface in the hatched region.

b) *Viscous dissipation.* As the line relaxes, at velocity $\dot{u}_q = \frac{\partial u_q}{\partial t}$, the liquid is put into motion. We assume that the rubber is purely elastic (in some cases the viscoelastic dissipation in the rubber can play a major role [22]) and we neglect the viscous dissipation at the contact line in the liquid wedge of size h_0. All the dissipation takes place in the liquid squeezed at the R/S interface (the liquid wedge contribution is smaller by a ratio $qh_0 \ll 1$). The same approximations used to describe the dynamics of the contact growth [19] have been confirmed experimentally for the same elastomer. Per unit length in the y-direction, the viscous dissipation is $T\dot{S} = \int\int \eta (\frac{\partial v}{\partial z})^2 \, \mathrm{d}x \, \mathrm{d}z$ (where $\dot{S}$ and $v \cong \dot{u}_q$ are, respectively, the entropy production rate and the velocity in the liquid). Here the integration $\int \mathrm{d}z$ takes place over the slit thickness $z_0(x)$ and the result is

$$T\dot{S} \cong \eta \dot{u}_q^2 (h_0 q)^{-1/2}. \tag{5}$$

Frequency spectrum of the "triplons". – The transfer of elastic energy $\mathrm{d}F_{el}/\mathrm{d}t$ into viscous dissipation $T\dot{S}$ leads to

$$-|S|qu_q \approx \eta \dot{u}_q (h_0 q)^{-1/2}. \tag{6}$$

Equation (6) shows that, for a mode corresponding to a wave number q with an amplitude deformation u_q, the amplitude deformation u_q should relax exponentially: $u_q = u_{q_0} e^{-t/\tau_q}$ with a relaxation time τ_q:

$$\tau_q \approx \frac{\eta}{|S|h_0^{1/2}q^{3/2}} \approx \frac{\eta E^{1/2}}{|S|^{3/2}q^{3/2}}. \tag{7}$$

This expression for τ_q suggests two remarks: i) τ_q increases with the elastic modulus. This result is surprising: soft systems are usually slower than hard ones. It can be explained by a larger viscous dissipation. Indeed, larger elastic modulus E corresponds to smaller elastic length h_0. The parabolic liquid surface profile is more flattened and the viscous dissipation increases. ii) This relaxation time predicted by eq. (7) is very different from that obtained in S/L/A triple lines in viscous regime [3], where the viscous dissipation inside a liquid wedge does not depend upon q.

Discussion. – We now compare our experimental results for the relaxation time to τ_q (given by eq. (7)):

i) *Relaxation time vs. wave vector.* The q-dependence is in rough agreement with the experimental results: we get the experimental relation $\tau_q \sim q^{-1.2\pm0.3}$, whereas eq. (7) predicts $\tau_q \sim q^{-1.5}$. The difference between both exponents is not very significant since our experiments cover only half a decade of q vectors.

ii) *Relaxation time vs. viscosity.* We observe that τ_q is nearly linear with the liquid viscosity η : $\tau_q \sim \eta^{1.1\pm0.3}$. This result is compatible with our model (which predicts $\tau_q \sim \eta$).

iii) Relaxation time vs. elastic modulus. In a qualitative way, we observe what theory expects: "soft" elastomers relax more quickly than "hard" ones. In a more quantitative way, "soft" elastomers relax more slowly than predicted. The ratio of the two measures of τ_q for $E = 0.8\,\mathrm{MPa}$ and $E = 0.2\,\mathrm{MPa}$ gives 1.6, instead of 2.0 predicted by the model. This might be explained by a hysteretic behavior of "soft" elastomers (observed in different experiments by Clain [23]). When compressing or decompressing a glass slide on a "soft" elastomer, slower velocities are observed for the contact zone when moving forward (compression) than backward (decompression) whereas for "hard" elastomers, both fronts move at the same velocity. In our case, when the triple-line relaxes, one front moves forward and the other moves back. This contribution tends to increase the relaxation time τ_q for "soft" elastomers.

Concluding remarks. – To our knowledge, we performed the first experiments on the relaxation of triple lines at soft interfaces, "soft triplons".

We found a way to study S/L/R triple line relaxation: we press a hydrophobic glass plate with indents row on it, through a PFAS drop, against a cylinder rubber. After the liquid dewetting, a relative displacement of the cylinder and the defects row generates triple line periodic undulations. This experimental set-up allows us to measure S/L/R relaxation time τ_q as a function of the liquid viscosity η and the wave vector q. We find the experimental relation $\tau_q \approx \eta^{1.1} q^{-1.2}$. We also change the elastic modulus E of the elastomer and observe that "soft" elastomers relax more quickly than "hard" ones.

We construct a scaling theory to explain these observations. It is based on a balance between elastomer elastic deformation and viscous losses in the liquid. It explains reasonably well our experimental data on the variation of the relaxation time τ_q *vs.* wave vector and viscosity. This model also explains why softer elastomers relax faster than hard ones. However we are limited to a narrow range of variation of the elastic modulus. For too soft rubbers, the velocity dependence of the peeling energy cannot be neglected and our approximation of dissipation inside the liquid only is not valid. Reinforced rubbers would allow to achieve higher E values. The modes of a contact line which have been observed here may also play a role for the fracture of a rubber immersed in a liquid [24].

$$* * *$$

REFERENCES

[1]   Joanny J.-F. and de Gennes P. G., *J. Chem. Phys.*, **81** (1984) 552.
[2]   de Gennes P. G., *Rev. Mod. Phys.*, **57** (1985) 827.
[3]   de Gennes P. G., Brochard-Wyart F. and Quéré D., *Capillary and Wetting Phenomena: Drops, Bubbles, Pearls, Waves* (Springer, 2003).
[4]   Brochard-Wyart F. and de Gennes P. G., *Langmuir*, **7** (1991) 3216.
[5]   Ondarçuhu T. and Veyssié M., *Nature*, **352** (1991) 418.
[6]   Ondarçuhu T., *Mod. Phys. Lett. B*, **6** (1992) 901.
[7]   Paterson A. *et al.*, *Phys. Rev. E*, **51** (1995) 1291.
[8]   Sauer B. B. and Carney T. E., *Langmuir*, **6** (1990) 1002.
[9]   Nadkarni G. D. and Garoff S., *Europhys. Lett.*, **20** (1992) 523.
[10] Di Meglio J. M., *Europhys. Lett.*, **17** (1992) 607.
[11] Marsh J. A. and Cazabat A. M., *Europhys. Lett.*, **23** (1993) 45.
[12] Poujade M., Guthmann C. and Rolley E., *Europhys. Lett.*, **59** (2002) 862.
[13] Noblin X., Buguin A. and Brochard-Wyart F., *Langmuir*, **18** (2002) 9350.

[14] MARTIN P. and BROCHARD-WYART F., *Phys. Rev. Lett.*, **80** (1998) 3296.

[15] MARTIN P., SILBERZAN P. and BROCHARD-WYART F., *Langmuir*, **13** (1997) 4910.

[16] ROBERTS A. D. and TABOR D., *Proc. R. Soc. London, Ser. A*, **325** (1971) 323.

[17] MARTIN A., BUGUIN A. and BROCHARD-WYART F., *Langmuir*, **17** (2001) 6553.

[18] VERNEUIL E., CLAIN J., BUGUIN A. and BROCHARD-WYART F., *Eur. Phys. J. E*, **10** (2003) 345.

[19] BROCHARD-WYART F. and DE GENNES P.-G., *J. Phys. Condens. Matter A*, **6** (1994) 9.

[20] SILBERZAN P. and LÉGER L., *Phys. Rev. Lett.*, **66** (1991) 185.

[21] BRZOSKA J. B., SHAHIZADEH N. and RONDELEZ F., *Nature*, **360** (1992) 24.

[22] SHANAHAN M. and CARRÉ A., *Nature*, **379** (1996) 432.

[23] CLAIN J., Thèse de doctorat, University Paris 6 (2004).

[24] DE GENNES P.-G., *C. R. Acad. Sci. Paris, Ser. II*, **304**, no. 11 (1987).